PAPER Special Section on Medical Information and Communications Technologies

SA and SAR Analysis for Wearable UWB Body Area Applications

Qiong WANG†, ***Student Member and*** **Jianqing WANG**†a), ***Member***

SUMMARY With the rapid progress of electronic and information technology, an expectation for the realization of body area network (BAN) by means of ultra wide band (UWB) techniques has risen. Although the signal from a single UWB device is very low, the energy absorption may increase significantly when many UWB devices are simultaneously adorned to a human body. An analysis method is therefore required from the point of view of biological safety evaluation. In this study, two approaches, one is in the time domain and the other is in the frequency domain, are proposed for the specific energy absorption (SA) and the specific absorption rate (SAR) calculation. It is shown that the two approaches have the same accuracy but the time-domain approach is more straightforward in the numerical analysis. By using the time-domain approach, SA and SAR calculation results are given for multiple UWB pulse exposure to an anatomical human body model under the Federal Communications Commission (FCC) UWB limit.
key words: *ultra wide band (UWB), specific energy absorption (SA), specific absorption rate (SAR), frequency-dependent finite difference time domain (FDTD) method*

1. Introduction

The ultra wideband (UWB) system is a promising candidate for the on-body communications, in view of its features of multi-path compensation, lower consume power, high transmission speed, and simple structure [1]. The IEEE 802.15.4a [2] has been developed as a low rate wireless personal area network (PAN) [3] UWB standard for various application to share the data, reduce functional redundancies and allow new conveniences and services. Moreover, wearable and implanted body area networks (BANs) are being developed for medical and health information monitoring [4]. For example, wearable health monitoring systems for medical check-up may be composed of EEG (electroencephalogram) sensors for monitoring brain electrical activity, ECG (electrocardiogram) sensors for monitoring heart activity, breathing sensors for monitoring respiration and blood pressure sensors and so on. The data from all of these sensors will be transmitted by wireless PAN or LAN to remote receivers. Although the signal from one UWB device is very low, however, it is unclear that the energy absorption will increase to what extent while many UWB devices are adorned simultaneously to a human body, which is exactly the actual situation for a body area network. An analysis method is therefore required from the point of view of biological safety evaluation.

Manuscript received April 14, 2008.
Manuscript revised August 13, 2008.
†The authors are with the Graduate School of Engineering, Nagoya Institute of Technology, Nagoya-shi, 466-8555 Japan.
a) E-mail: wang@nitech.ac.jp
DOI: 10.1587/transcom.E92.B.425

In this paper, two approaches are proposed to calculate the specific energy absorption (SA, defined as the energy absorbed per unit mass of biological body) for UWB pulse exposure. Both the two approaches are based on a frequency-dependent finite difference time domain (FDTD) method, in which the Debye approximation is used to represent the frequency-dependent dielectric properties of the human body and the SA is calculated for a single UWB pulse excitation. Then the specific absorption rate (SAR, defined as the power absorbed per unit mass of biological body) is derived based on UWB modulation schemes. In this study, two representative schemes, one is the impulse radio (IR) scheme and the other is the direct sequence spread spectrum (DS-SS) scheme, are considered, and the SA and SAR is analyzed with an emphasis on multiple UWB device exposure.

2. Analysis Method and Human Modeling

The time-domain Maxwell curl equations are

$$\nabla \times E(t) = -\mu \frac{\partial H(t)}{\partial t} \tag{1}$$

$$\nabla \times H(t) = \frac{\partial D(t)}{\partial t} + J_0(t) \tag{2}$$

where the electric flux density D is related to the electric field E through the complex permittivity of human body tissue. Assuming that the complex relative permittivity of a human tissue can be approximated by the Debye equation [5]

$$\varepsilon_r(\omega) = \varepsilon_\infty + \chi(\omega) + \frac{\sigma_0}{j\omega\varepsilon_0} \tag{3}$$

where ε_0 is the permittivity of free space, ε_∞ is the relative permittivity at infinite frequency, $\chi(\omega)$ is the frequency-domain susceptibility, and σ_0 is the static electric conductivity, we can relate the first and second terms in Eq. (3) to $D(\omega)$ and the third term to $J_0(\omega)$ because only the former two terms are due to the frequency dispersion of tissue. We therefore have

$$D(\omega) = \varepsilon_0 \left[\varepsilon_\infty + \chi(\omega)\right] E(\omega) \tag{4}$$

$$J_0(\omega) = \sigma_0 E(\omega). \tag{5}$$

Since Eqs. (1) and (2) are to be solved iteratively in the time domain by using the FDTD method, we need to transfer Eqs. (4) and (5) into the time domain. This can be realized by Fourier transform. We thus have

$$D(t) = \varepsilon_0 \varepsilon_\infty E(t) + \varepsilon_0 \chi(t) * E(t) \quad (6)$$

$$J_0(t) = \sigma_0 E(t) \quad (7)$$

where the symbol * denotes the convolution. We can use Eq. (6) and (7) to derive a frequency-dependent FDTD algorithm, as described in [5], [6] in detail, for calculating the electric field inside and around the human body.

For the human body model used for the SA and SAR analysis, we employ a Japanese adult male model [7]. As shown in Fig. 1, the model has been developed based on magnetic resonance imaging data. It has a height of 173 cm, a weight of 65 kg, and a spatial resolution of 2 mm. It consists of 51 tissue types. For incorporating the tissue properties into the frequency-dependent FDTD method, we assume one-relaxation Debye approximation, i.e.,

$$\chi(\omega) = \frac{\varepsilon_s - \varepsilon_\infty}{1 + j\omega\tau} \quad (8)$$

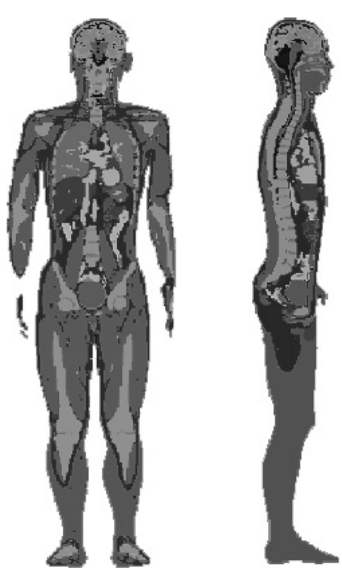

Fig. 1 Anatomically based human body model (Male, 173 cm, 65 kg).

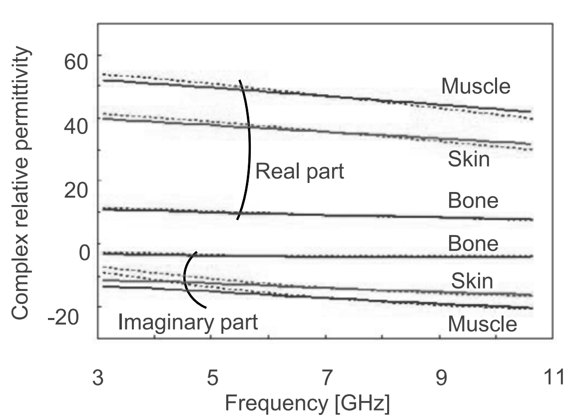

Fig. 2 Fitted complex relative permittivity values for muscle, skin and bone as a function of frequency.

in Eq. (3), and determine the parameters ε_s, ε_∞ and τ for all of the 51 tissue types. Assuming Gabriel's measurement-based data [8] as the true values, we determine these parameters by using the least square error fitting in the UWB frequency band from 3.1 to 10.6 GHz. Figure 2 shows the fitted complex relative permittivity values for muscle, skin and bone as a function of frequency. The imaginary parts are negative in mathematics. The straight lines are measurement-based data, and the broken lines are one-relaxation Debye approximation. They have fair agreement at this frequency band between 3.1 to 10.6 GHz. Figure 3 shows the fitting errors averaged over the entire frequency band for all of the tissues in the human body model. The average difference is found to be within ±10% between the one-relaxation Debye approximation and measurement-based data in the considered frequency band. Moreover, the maximum difference at any frequency between 3.1 to 10.6 GHz is within ±20% for all of the 51 tissues. Although a second-order [9] or high-order Debye relaxation approximation [8] offers the advantage of better fit to the measurement data, the one-relaxation Debye approximation has a reasonable accuracy.

3. SA and SAR Calculation Method

According to the definition of Federal Communications Commission (FCC) [10], the UWB signal is defined as such a signal that has a ratio of the bandwidth to the center frequency larger than 0.2, or a bandwidth larger than 500 MHz. As a UWB antenna, we choose an elliptic disk dipole with a major axis of 25 mm diameter and a minor axis of 21 mm diameter, which yields a voltage standing wave ratio (VSWR) nearly 2.0 between 3.1 and 10.6 GHz. As a UWB pulse to be transmitted, we choose a 5th-derivative Gaussian pulse with a pulse width of nearly 500 ps. Figure 4 shows the employed 5th-derivative Gaussian pulse waveform and the equivalent isotropically radiated power (EIRP). The EIRP is derived as follows. In general,

$$EIRP = P_a G_a \quad (9)$$

where P_a is the power supplied to the UWB antenna and G_a is the absolute gain of antenna. The determination of P_a depends on the UWB modulation scheme. For the UWB-IR or DS-SS scheme, we can first calculate the antenna power density

$$P_{SD}(f) = Re[V(f)V^*(f)/Z_{in}(f)]/T \quad (10)$$

where $V(f)$ is the Fourier transform of the UWB pulse voltage with unit of V/Hz, $Z_{in}(f)$ is the antenna input impedance and T is the pulse duration. Then we have the EIRP as

$$EIRP[dBm/MHz] = 10\log_{10}[2P_{SD}(f)] + 10\log_{10} G_a + 90 \quad (11)$$

It can be found from Fig. 4 that the maximum power of the employed 5th-derivative Gaussian pulse is limited to −41.3 dBm/MHz between 3.1 and 10.6 GHz, i.e., it meets

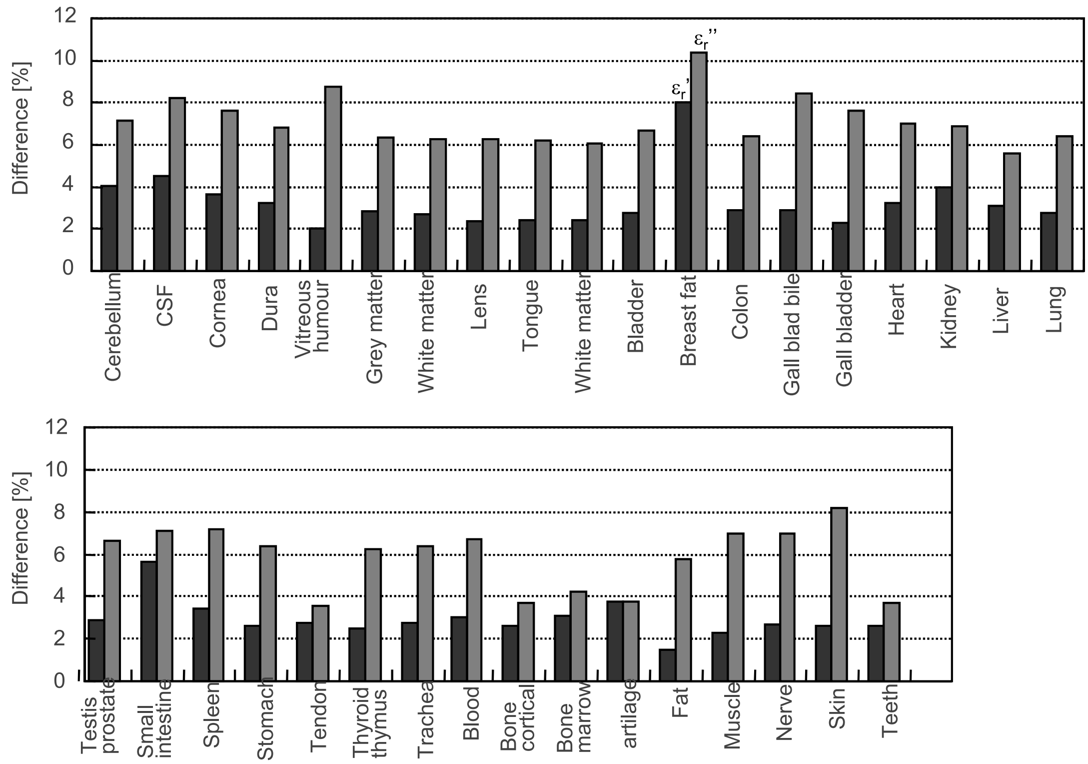

Fig. 3 Fitting errors averaged over the entire frequency band of 3.1 to 10.6 GHz for all of the tissues in the human body model.

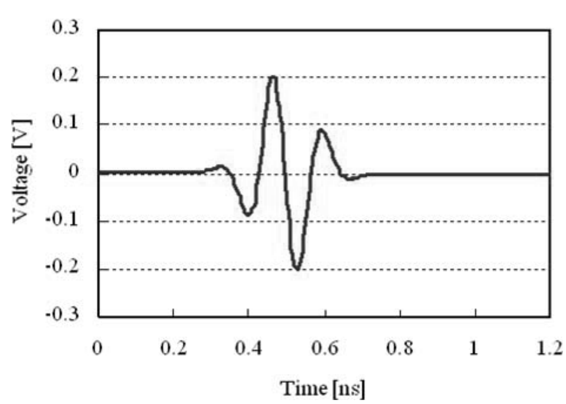

(a)

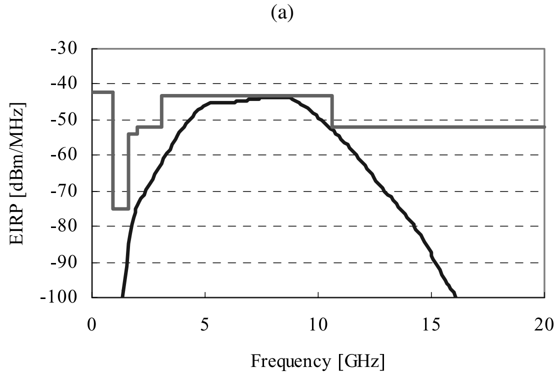

(b)

Fig. 4 (a) 5-th derivative Gaussian pulse waveform; (b) FCC indoor emission spectrum mask and the equivalent isotropically radiated power.

with the FCC indoor emission spectrum mask. Under the FCC UWB limit, we perform the SA and SAR calculation for the anatomical human body model. At first, we investigate the validation of two approaches for the SA calculation. The first approach is to calculate the current density in the time domain in the frequency-dependent FDTD method, i.e.,

$$J(t) = \sigma_0 E(t) + \varepsilon_0 \frac{d}{dt}[\chi(t) * E(t)] \tag{12}$$

Then we obtain the SA from

$$SA = \int_0^T J(t)E(t)/\rho \cdot dt \tag{13}$$

where ρ is the mass density. This calculation is straightforward in the frequency-dependent FDTD method, and it does not need additional calculation burden.

The second approach is the frequency domain expression of the first approach. According to Parserval theorem,

$$SA = \int_{-\infty}^{\infty} \sigma(\omega) \mid E(\omega) \mid^2 /\rho \cdot df \tag{14}$$

where $\sigma(\omega) = -\omega\varepsilon_0 Im[\varepsilon_r(\omega)]$ is the lossy component of the dielectric properties and $E(\omega)$ is the Fourier transfer of $E(t)$. We get $E(\omega)$ directly in the frequency-dependent FDTD method as a running summation at each time step based on the discrete Fourier transfer. This approach requires additional calculation burden.

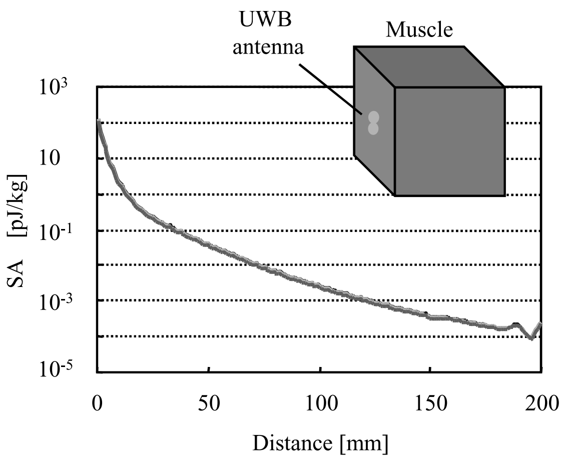

Fig. 5 Calculated SA profile taken from the front to the back of the muscle cube. The two approaches give the completely same SA values.

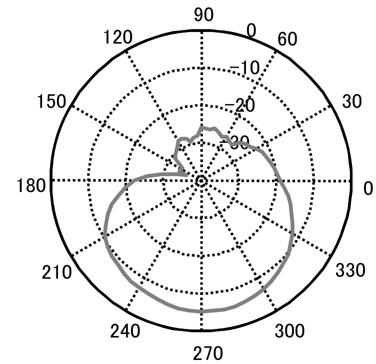

Fig. 6 Antenna radiation pattern in the horizontal plane at 5 GHz.

We compare the SA calculation results by using the two approaches. Although the two approaches are mathematically equivalent, the corresponding numerical algorithms are different. Comparison of the calculation results between the two approaches can confirm the validation of the time-domain algorithm which will be employed in the follow-up SA and SAR calculations.

A UWB antenna is placed in the front of a cube, parallel to the body surface. The UWB antenna is an elliptic disc dipole antenna with a major axis radius a and a minor axis radius b, that are determined as a = 12.5 mm and b = 10.5 mm in order to obtain a voltage standing wave ratio (VSWR) of below 2.0. The cube has a length of 200 mm and the dielectric properties of muscle. Fig. 5 shows the calculated SA profile taken from the front to the back of the muscle cube. As can be seen, both the first and the second approaches give the same SA values. In view of the calculation efficiency, the first approach in the time domain is more appropriate to the SA calculation in the frequency-dependent FDTD method.

4. SA and SAR Results and Discussion

We then use the first approach to calculate the SA for the UWB antenna placed on the body area such as the chest, ear, eye and waist. Figure 6 shows the antenna radiation pattern in the horizontal plane at a central UWB frequency of 5 GHz in the situation that the UWB antenna is placed on the chest. It can be seen that the power radiates towards the front or the outside of the body. Similar radiation pattern can be also observed in other situations. In the single exposure case, the UWB antenna is placed in one of the four locations, and in the multiple exposure case, two or four UWB antennas are simultaneously placed in two of or all of the four locations. The antenna input pulse is set to have the EIRP just under the FCC limit for UWB signal, i.e., −41.3 dBm/MHz. Figuer 7 shows the SA distributions on the body surface for both single and multiple UWB pulse exposure. The 0 dB corresponds to 10 pJ/kg. As can be seen, the SA concentrates on very small area on the body surface near the UWB antenna location, and the attenuation is more than 30 dB at a location 10 cm far from the UWB antenna. Especially, in the multiple-exposure situation the enhancement effect from neighbor UWB antenna is not obvious. This may be at-

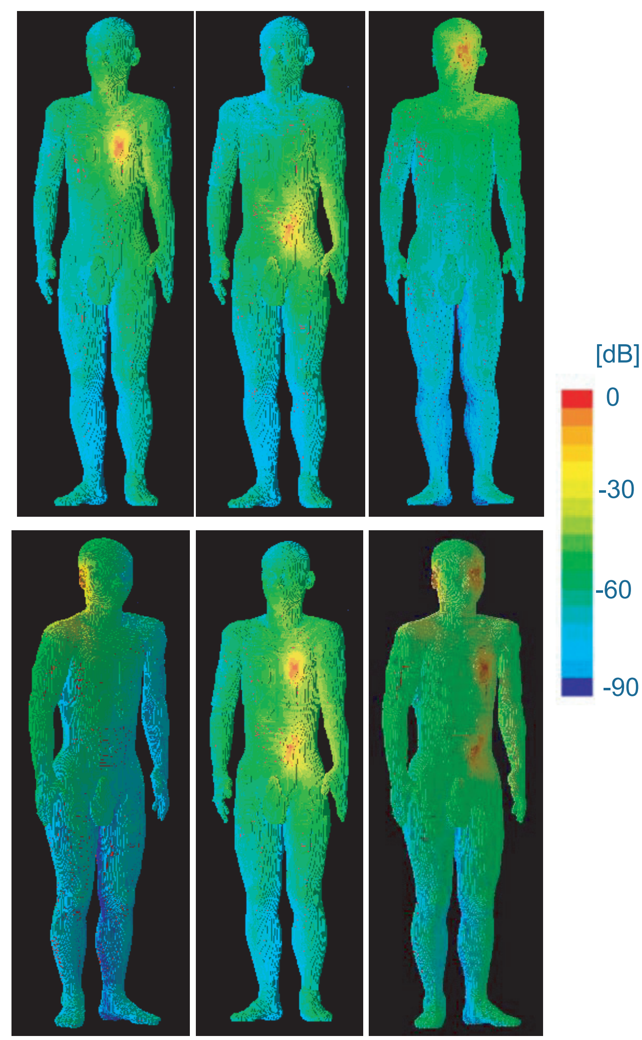

Fig. 7 SA distributions under the FCC UWB limit for various antenna locations. The 0 dB corresponds to 10 pJ/kg.

Table 1 Ten-gram averaged SA and SAR under FCC UWB limit.

Antenna Location	Peak SA [pJ/kg]	10g SA [pJ/kg]	10 g SAR [mW/kg]
Chest	7.00	0.473	0.946
Ear	2.17	0.037	0.074
Eye	13.26	0.268	0.536
Waist	7.39	0.232	0.464
Multiple exposure			
Chest+Waist	7.40	0.474	0.948
Chest+Ear+Eye+Waist	13.27	0.476	0.952

tributed to the rapid attenuation of the UWB signal on the body surface.

For the IR and DS-SS modulation of UWB signals, the SAR can be simply obtained from the ratio of SA to the pulse duration T. That is, SAR = SA/T. Of course UWB pulse should be repeated for communication usages. For SA, it is generally evaluated on single pulse. For SAR, however, the values for single pulse and for pulse series are the same because the SAR is the ratio between SA and T for the above-mentioned modulation schemes. That is to say, the quantities for SA and T will increase simultaneously N times for a series of N pulses. It is therefore reasonable to use single pulse to investigate the SA and SAR.

Table 1 gives the peak SA, the ten-gram-averaged SA and the ten-gram-averaged SAR in all of the six situations as shown in Fig. 7. As can be seen from Table 1, compared to single exposure, almost no obvious increase in the SA and SAR are observed in the multiple exposure cases. This suggests that as long as the separation between two UWB devices is larger than 30 cm, the additional effect of signals from other devices is insignificant due to the rapid surface attenuation of UWB signals. In order to verify this conclusion furtherly, we observed the E-field at the chest under multiple exposure and the result is shown in Fig. 8. Since the separation distance between other devices and the device at the chest is about 30 cm, the transmission time is at least 1 ns. It means that if the effect of signals from other devices is not negligible, there should be some significant components around 1 ns in the observed E-field. This does not depend on whether the devices are excited simultaneously or un-simultaneously. From Fig. 8, no significant component is observed around 1 ns. The conclusion is therefore drawn that the E-field attenuates very quickly and the effect of other signal becomes negligible.

The ten-gram-averaged SA is in the order of pJ/kg and is much smaller than the ICNIRP safety guideline of 2 mJ/kg. The ten-gram-averaged SAR is in the order of mW/kg and is smaller than 1/2000 of the ICNIRP safety guideline of 2 W/kg [11]. The energy absorbed by the whole body is found to be 0.01 pJ which is about a quarter of the energy radiated from the antenna.

The SA and SAR varies with the distance between the antenna and the human body. Table 2 shows the 10 g-averaged SA and SAR corresponding to distances of 2 mm, 1 cm and 2 cm when one UWB antenna is adorned on the chest. It can be seen from the table that the 10 g-averaged

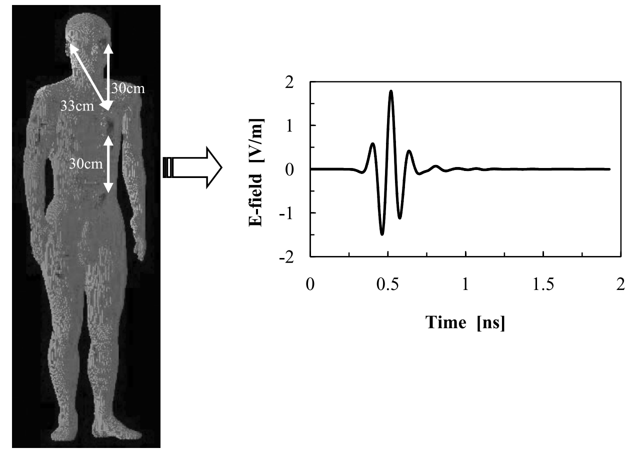

Fig. 8 Distance separation and E-field at the chest (at 1cm above chest surface) under multiple exposure.

Table 2 Ten-gram averaged SA and SAR with different antenna distance from body.

Antenna Location (distance from chest)	10 g SA [pJ/kg]	10 g SAR [mW/kg]
2 mm	0.473	0.946
1 cm	0.034	0.068
2 cm	0.013	0.026

SA and SAR values will decrease by 12 dB and 17 dB respectively when the distances become 1 cm and 2 cm compared with the initial distance of 2 mm. In practice, the antenna will be adorned as closely as possible to the body surface. Therefore, the 2 mm case we calculated may represent the worst case. The further the distance becomes, the larger the safety margain there will be.

5. Conclusion

The UWB system is a promising candidate for the on-body communications in view of its features of small power and multi-path compensation. However, it is unclear that the energy absorption will increase to what extent when many UWB devices are adorned to a human body. An analysis method is therefore necessary from the point of view of biological safety evaluation. In this paper, using the FDTD method, we have proposed two approaches to calculate the SA and SAR for UWB pulse exposure. We have shown that the two approaches have the same accuracy but the time-domain approach is more straightforward to the SA and SAR analysis for IR and DS-SS modulation scheme. We have also demonstrated the SA and SAR levels under the FCC UWB limit for various antenna locations on an anatomical human body model. The results have shown that the SA and SAR levels are much smaller than the IEEE safety limits and the multiple exposure does almost not obviously increase the SA and SAR as long as two UWB devices have a separation as large as 30 cm.

Acknowledgement

This study was supported by Telecom Engineering Center, Japan.

References

[1] M. Ghavami, L.B. Michael and R. Kohno, "Ultra Wideband Signals and Systems in Communication Engineering," John Wiley & Sons, England, 2004.
[2] http://www.ieee802.org/15/pub/TG4a.html
[3] T.G. Zimmerman, "Personal area networks: Near-field intrabody communications," IBM Syst. J., vol.35, nos.3&4, pp.609–617, 1996.
[4] http://grouper.ieee.org/groups/802/15/pub/Subscribe.html
[5] K.S. Kunz and R. Luebbers, The Finite Difference Time Domain Method for Electromagnetics, CRC Press, Boca Raton, 1993.
[6] F.S. Barnes and B. Greenebaum, Bioengineering and Biophysical Aspects of Electromagnetic Field, CRC Press, 2006.
[7] T. Nagaoka, S. Watanabe, K. Saurai, E. Kunieda, S. Watanabe, M. Taki, and Y. Yamanaka, "Development of realistic high-resolution whole-body voxel models of Japanese adult males and females of average height and weight, and application of models to radio-frequency electromagnetic-field dosimetry," Phys. Med. Biol., vol.49, pp.1–15, 2004.
[8] C. Gabriel, "Compilation of the dielectric properties of body tissues at RF and microwave frequencies," Brooks Air Force Technical Report AL/OE-TR-1996-0037, 1996.
[9] O.P. Gandhi and C.M. Furse, "Currents induced in the human body for exposure to ultrawideband electromagnetic pulses," IEEE Trans. Electromagn. Compat., vol.39, no.2, pp.174–180, May 1997.
[10] FCC 02-48, "Revision of part 15 of the commission's rules regarding ultra-wideband transmission systems," 2002.
[11] ANSI/IEEE Std C.95.1, "Safety levels with respect to human exposure to radio frequency electromagnetic fields — 3 kHz to 300 GHz," 1992.

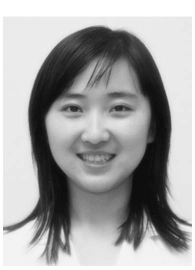

Qiong Wang received the B.E. degree in communication engineering from Yanshan University, China, in 2003. From 2003, she has been working for her Ph.D. degree in Department of Electrical Information Engineering, Beijing University of Aeronautics and Astronautics, Beijing, China. She is currently engaged in the study of on-body area communications and biomedical EMC towards the Ph.D. degree in Nagoya Institute of Technology, Nagoya, Japan.

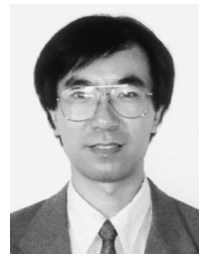

Jianqing Wang received the B.E. degree in electronic engineering from Beijing Institute of Technology, Beijing, China, in 1984, and the M.E. and D.E. degrees in electrical and communication engineering from Tohoku University, Sendai, Japan, in 1988 and 1991, respectively. He was a Research Associate at Tohoku University and a Senior Engineer at Sophia Systems Co., Ltd., prior to joining the Nagoya Institute of Technology, Nagoya, Japan, in 1997, where he is currently a Professor. His research interests include biomedical communications and electromagnetic compatibility.